TREATMENT OF HIGHLY VISCOUS LUBRICANTS BY HIGH GRADIENT MAGNETIC SEPARATION

Katharina Menzel (katharina.menzel@kit.edu), Johannes Lindner and Hermann Nirschl
Institute of Mechanical Process Engineering and Mechanics (MVM), Karlsruhe Institute of Technology, 76131 Karlsruhe, Germany.

Abrasive particles in gear and hydraulic oils are responsible for increased wear in machine elements like bearings or the breakdown of entire machine systems, e.g. the gears in wind power plants. The monitoring of the lubricant condition as well as its continuous treatment is therefore essential to increase the lifetime of the equipment[1]. The separation of micrometre particles ranging from 1 to 20 µm of a high viscosity lubricant is still challenging in state-of-the-art deep bed filtration because of high pressure drop and the unintentional separation of additives. Wear particles of different chemical composition are magnetisable and therefore magnetic separation is a promising approach to separate these particle clusters, while avoiding the separation of oil additives. The magnetic force is effective at great distance from the separating wire. The HGMS filter is therefore configured to be more porous than a conventional filter material. Hence, the pressure drop in High Gradient Magnetic Separation (HGMS) is negligible which is a great advantage and helps to decrease operating expenses.

INTRODUCTION

At the Institute of Mechanical Process Engineering and Mechanics a regenerative magnetic separator based upon the HGMS principle has been developed[2]. The method utilizes the magnetic force which is excited through the distortion of the external magnetic field by ferromagnetic wires. Next to the wire high magnetic forces occur, causing magnetisable particles to adhere to it. The filtration effect of an HGMS apparatus has similarities with deep bed filtration, although the principle has further important benefits. The application of thin wires ensures the separation of small magnetisable particles of micrometre and sub-micrometre scale. The magnetic force is effective even at a great distance from the wire (between 1 and 100 times the wire radius). Simultaneously, the porosity of the magnetic filter is significantly higher than that of a common deep bed filter. This allows any additives in the lubricating oil to pass unhindered, whereas they may be unintentionally separated in deep bed filters.

This paper presents the performance of the magnetic separator with regard to the deposition of particles on two different diameter wires and separation efficiency as a function of the flow and magnetic field strength of various single wire stages. The results show the loading distribution of the matrix stages dependent on their position within the HGMS filter apparatus. Another observation shows the separation grade of two different matrix arrangements.

METHOD

The separation apparatus, which is shown in a demounted state in Figure 1, has a flexible design in order to embed either a conventional filter or magnetisable HGMS filter elements (see Figure 2). The designated number of HGMS filter elements were assembled inside the apparatus. The distance between each

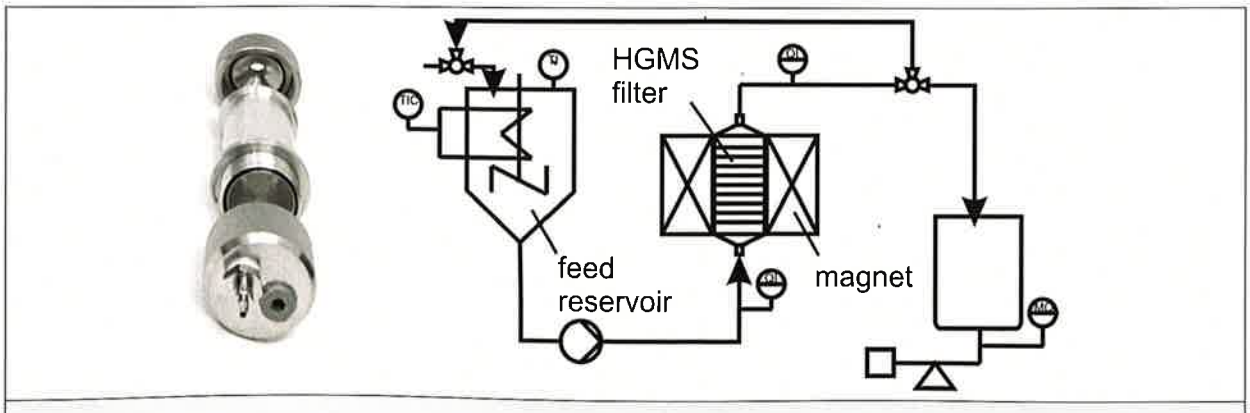

Figure 1: Separation device in demounted state (*left*) and test flow diagram (*right*).

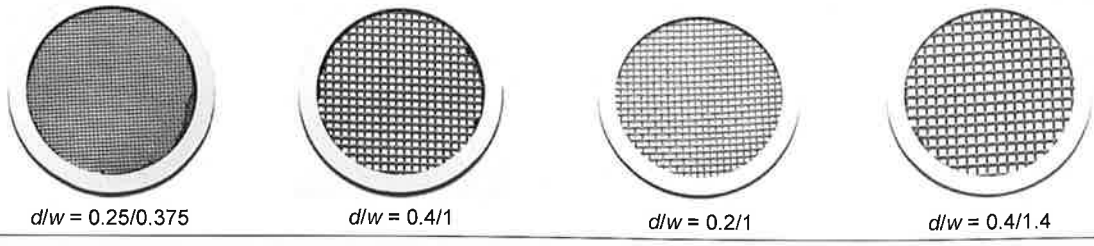

Figure 2: HGMS wire mesh stages with diameter of the wire d and mesh width w in mm.

filter element could be varied. A schematic diagram of the system is shown on the right side of Figure 1. The initial suspension was located inside a heated and stirred feed reservoir. The peristaltic pump fed the suspension into the HGMS filter located in the centre of an electromagnetic coil. In a single-pass test the fluid flowed into the collecting tray, where the weight was measured using a balance. In a multi-pass test the suspension was pumped in a closed loop as this is the way that filters are utilised in industrial oil circuits.

For the trials, wire mesh stages of magnetic ferrite stainless chromium steel DIN 1.4016 were produced. Their internal diameter was 30 mm and they are characterized by the wire diameter d and the mesh width w, with the notation being d/w and measurements in millimetres, e.g. (0.2/1). In the context of the wire mesh geometry the dimensionless specific surface area φ is introduced as an additional parameter for comparison between the mesh stages. It is defined as[3]:

$$\varphi = d\frac{A_S}{V} = d\frac{\pi l_D}{(w+d)^2} \approx \frac{\pi d\sqrt{d^2+(w+d)^2}}{(w+d)^2} \qquad (1)$$

where A_S is the surface area of the wire mesh, V the volume of the mesh and l_D the wire length. The dimensionless specific surface area φ can be expressed by the diameter of the wire d and the mesh width w if the interweavement of the wire is neglected (Figure 3). The dimensions of the matrices and their dimensionless specific surface area φ are shown in Table 1.

Deposition on the filter matrix element was determined gravimetrically. After completing the test, the oil in the filter cartridge was emptied and the filter matrix elements placed separately into bowls. Subsequently, the particles were detached from the elements using solvent in an ultrasonic bath and the resultant solvent suspension was filtered through a 0.2 µm membrane filter. The weight of the membrane was determined before and after filtration using a high precision balance. The separation efficiency was defined as

$$E = 100\left(1-\frac{C_{filtrate}}{C_{filtrate}}\right) \qquad (2)$$

where c is the concentration of the feed and filtrate, respectively. The separation grade G indicates the separation efficiency as a function of the particle size x. Using G it is possible to determine which particles of a given size fraction are separated and which remain in the filtrate. G is defined as:

$$G(x_m) = 100\left(1-\frac{q_{3,filtrate}(x_m)}{q_{3,feed}(x_m)}f\right) \quad \text{with } f = \frac{c_{filtrate}}{c_{feed}} \qquad (3)$$

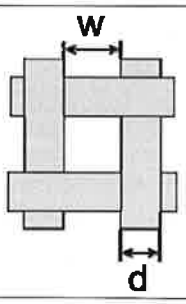

Figure 3: Wire mesh geometry.

Wire mesh	Wire diameter, d (mm)	Mesh width, w (mm)	Dimensionless specific surface area, φ (-)
0.25/0.375	0.25	0.375	1.35
0.4/1	0.40	1.000	0.93
0.4/1.4	0.40	1.400	0.72
0.2/1	0.22	1.000	0.53

Table 1: Dimensions of the HGMS filter matrix elements.

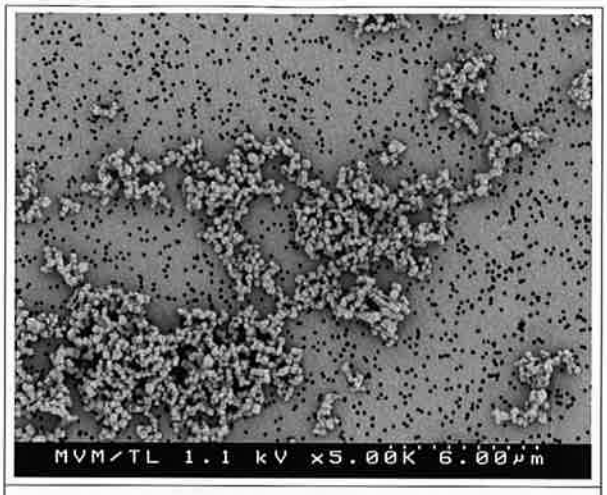

Figure 4: Scanning electron microscopy image of Bayoxid E8709 particles.

with the volume density distribution q_3 as a function of the equivalent median particle diameter x_m of the feed and filtrate, respectively. f is the filtrate proportion, hence the ratio of the particle concentration in the filtrate to that in the feed.

MATERIALS

The filtration of micrometre and sub-micrometre particles is a sophisticated task in deep bed filtration. Thus, the test material Bayoxid E8709 particles (LANXESS) was selected which consists of pure synthetically produced magnetite (Fe_3O_4). Its properties are listed in Table 2. The SEM image shown in Figure 4 demonstrates that the particle shape is partly round and rectangular and that they form large aggregates. The measurement of particle size is by laser light diffraction. The volume density distribution q_3 of magnetic particles is shown in Figure 5 where an average diameter of 3.5 µm is evident.

Mineral oil (Weber Reference Oils) FVA2 was used as the test media. The oil had no additives and was available as the reference oil. It was chosen because its viscosity at the test temperature of 20°C corresponds to that of the gear oil at its operating temperature of 60°C. The density of the oil is 866 kg/cm^3 at 20°C. Figure 6 shows the viscosity measurements as a function of temperature (from 10-30°C) where it can be seen that viscosity decreases when the temperature rises. Using an Arrhenius approach the dynamic viscosity η can be calculated as a function of the temperature t:

$$\eta = \eta_0 + A_1 \exp(-t/b) \qquad (4)$$

where the constants η, A_1 and b as determined for the oil are provided in Figure 6.

RESULTS

Deposition of Magnetic Particles on a Single Wire

The deposition of magnetic particles on a single wire as observed using an endoscopic video camera is shown in Figure 7. The left image in Figure 7 shows a longitudinally taut wire on which particles are deposited at the bottom and on the top. The pictures on the

Saturation magnetisation (A m²/kg)	Density (kg/m³)	BET specific surface area (m²/g)
94	5090	5.94

Table 2: Characteristics of the Bayoxid E8709 particles.

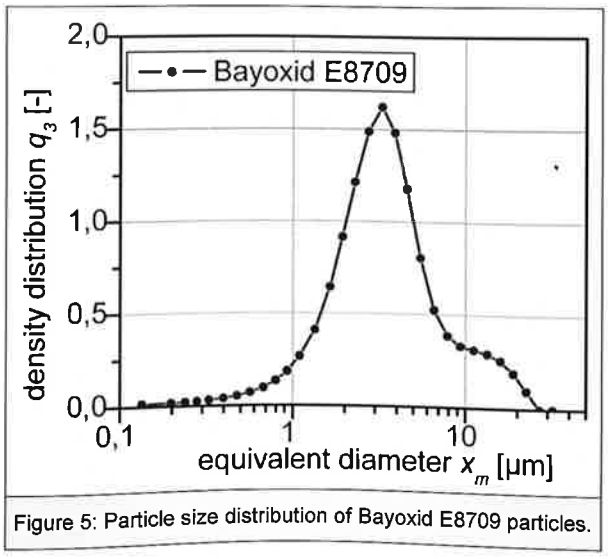

Figure 5: Particle size distribution of Bayoxid E8709 particles.

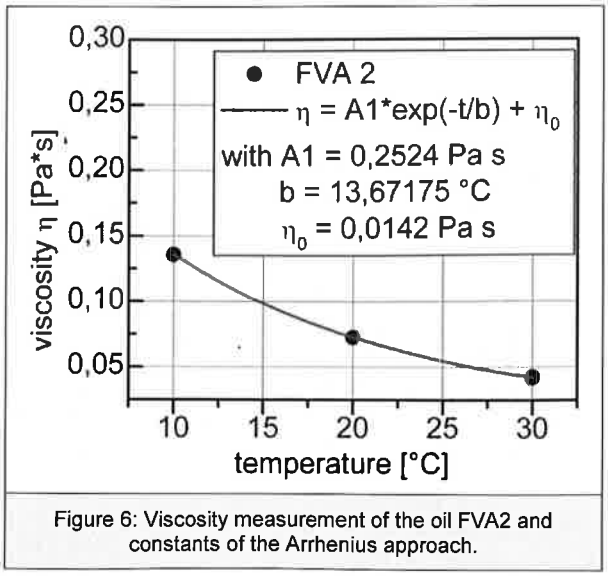

Figure 6: Viscosity measurement of the oil FVA2 and constants of the Arrhenius approach.

right side in Figure 7 show a wire cross section at the beginning of deposition (*left*) and at the time of saturation loading (*right*). At the time of saturation, the additional thickness was determined for a wire of radius 0.1 mm and 0.25 mm; the variation with the volumetric flow is shown in Figure 8. Here, it is evident that the particle loading on the thin wire (rectangular symbols) is less than on the thicker wire (triangular symbols) which means that the specific mass loading capacity of the wire increases for larger radius.

Single Filter Matrix Stage

The performance of the magnetic separator with regard to separation efficiency as a function of the flow and magnetic field strength was evaluated using a single wire stage. The experiments were conducted in single-pass and the filtered volume was kept constant. A single wire mesh stage was arranged in the centre of the filter apparatus.

The volume flow and the magnetic field density were varied in the experiments whilst the particle concentration of the feed was kept constant at 100 mg/l. In Figure 9, it is seen that the separation efficiency decreases as the flow rate increases from 10 to 50 ml/min at constant magnetic flux density (B = 0.12 T). Raising the magnetic field density B from 0.06 to 0.24 T at a constant volume flow of 30 ml/min causes the separation efficiency to increase (see Figure 10).

The loading distribution of an HGMS assembled with several matrix stages is important in order to be able to optimize the separation wire geometry. Figure 11 shows the deposited mass on each of the ten matrix steps along the filter length. The loading of the wire mesh at the inlet of the filter is the highest and declines in the direction towards the outlet. The difference be-

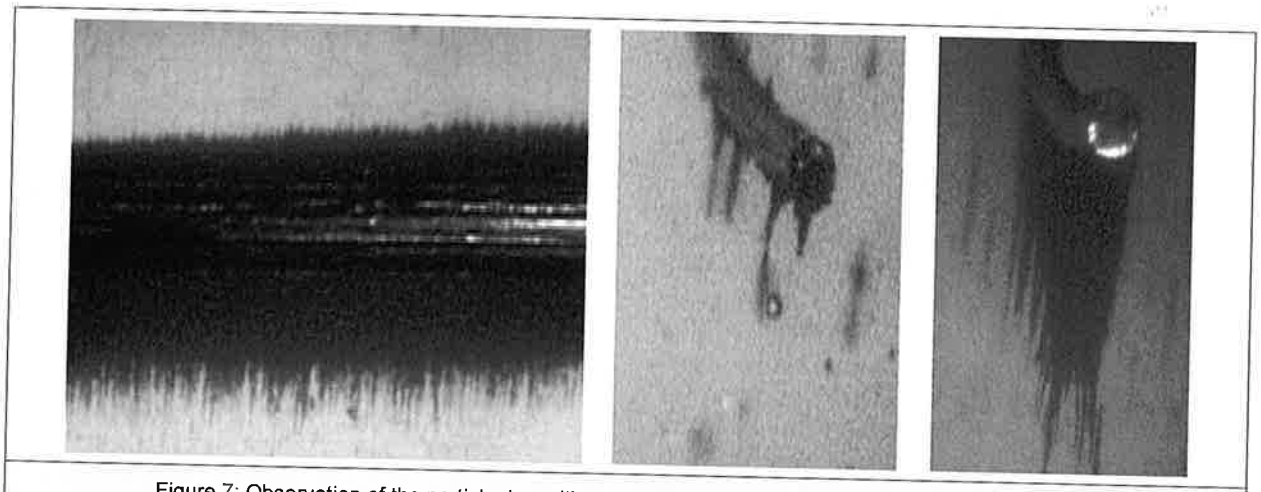

Figure 7: Observation of the particle deposition on a single wire using an endoscopic video camera.

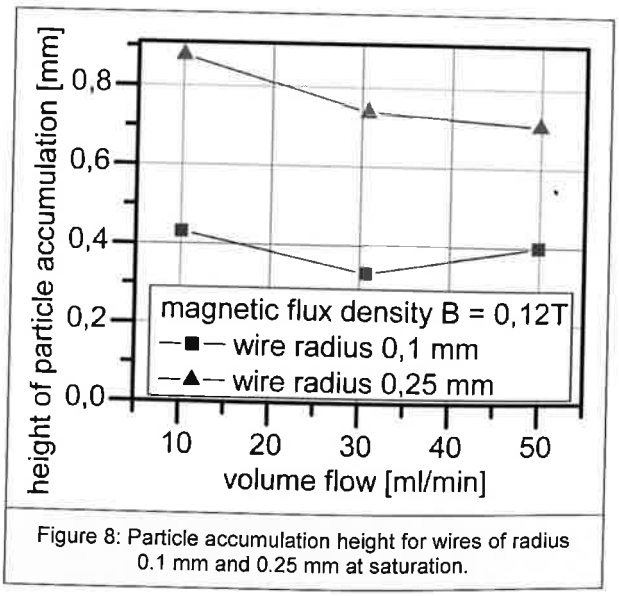

Figure 8: Particle accumulation height for wires of radius 0.1 mm and 0.25 mm at saturation.

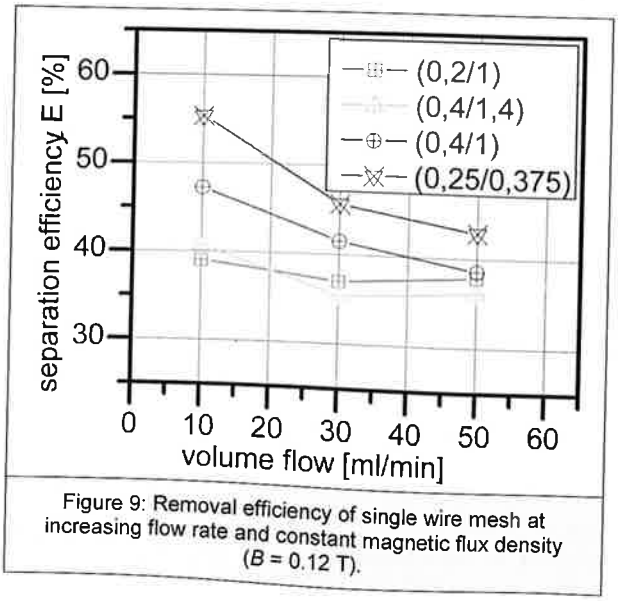

Figure 9: Removal efficiency of single wire mesh at increasing flow rate and constant magnetic flux density (B = 0.12 T).

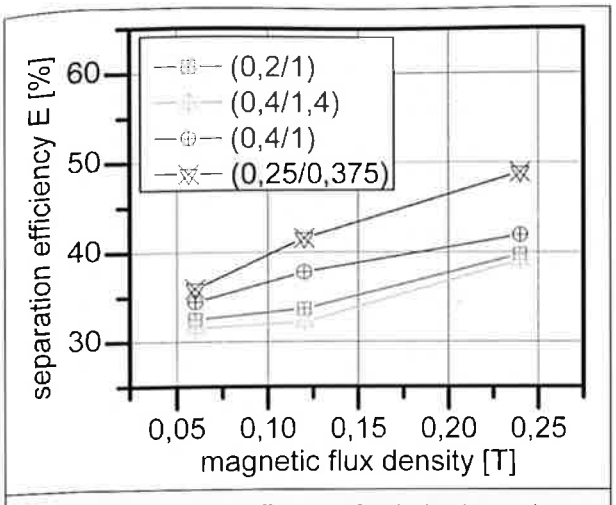

Figure 10: Removal efficiency of a single wire mesh at increasing magnetic flux density and constant flow rate (30 ml/min).

tween the mesh geometries can be seen where increasing dimensionless specific surface area φ of the wire mesh induces that the load grows.

The above results show the integral mass deposited on the wire mesh or the integral separation efficiency of the respective test. The grade efficiency gives the separation efficiency in dependency of the particle size. In Figure 12, the density distribution q_3 of the particles in the feed and the density distribution q_3 multiplied by the filtrate proportion f from the filtrate for two different experiments with one and ten mesh stages, respectively, are shown. The density distribution of particles in the feed shows that there are particles ranging from 0.5 to 80 µm. The experiment with a single mesh stage (circular symbols) shows that the proportion of smaller sized particles declines sharply compared to the feed curve (square symbols). Simultaneously, the proportion of particles larger than 20 µm increased which shows that the separation is inadequate if only one mesh stage is used. The magnetic gradient field inside the separation chamber causes enlargement of the particles by a magnetically induced agglomeration.

Increasing the number of mesh stages to ten, which are mounted vertically in the filter such that the mesh stage spacing is 5 mm, enables removal of the largest particles. The curve marked with the triangular symbols shows that all particles larger than 18 µm are almost completely separated. In order to separate the remaining particles the number of grid levels has to be increased further. The grade efficiency curves in Figure 13 complement the above observations.

CONCLUSIONS

The separation experiments using a single wire matrix stage show that the separation efficiency depends to a large extent on the geometry of the wire mesh. Increasing the dimensionless specific surface area φ of the wire matrix leads to enhancement of the separation efficiency. The experiments show that improving the separation efficiency of magnetic particles is achieved by reducing the velocity of the fluid and increasing the magnetic flux density of the background magnetic field. The number of wire matrix stages improves the separation efficiency. The first stage separates most of the particles. The measured size distributions of feed and filtrate show that the deposition and separation efficiency of one mesh stage is insufficient and causes enlargement of the particles by magnetically induced agglomeration. By increasing the number of stages to

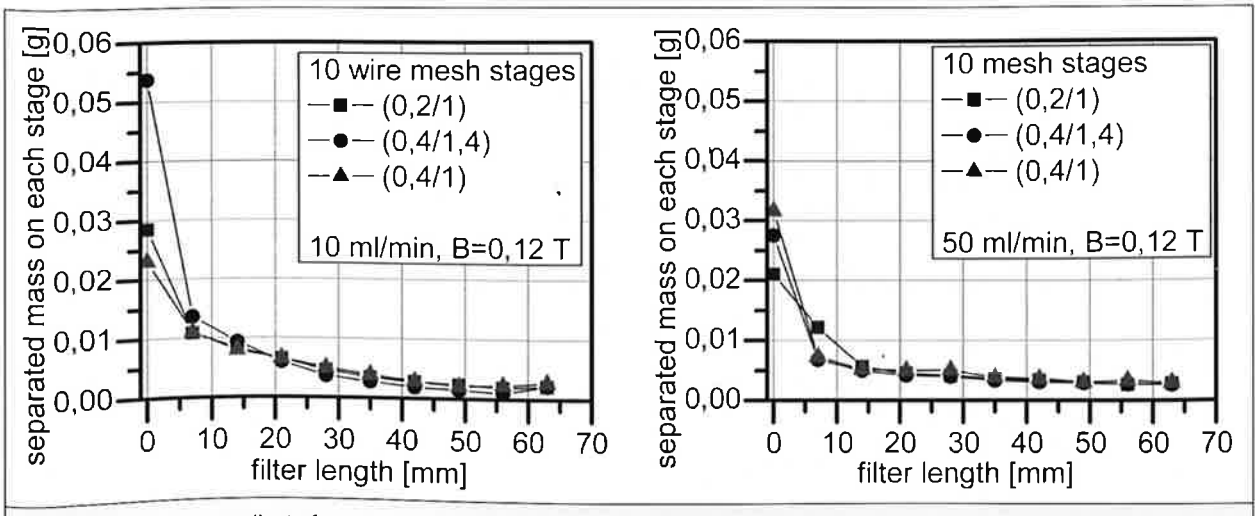

Figure 11: Loading gradient of mesh stages as a function of their position in the filter and size of the wire diameter, d, and mesh size w; 10 ml/min (*left*), 50 ml/min (*right*).

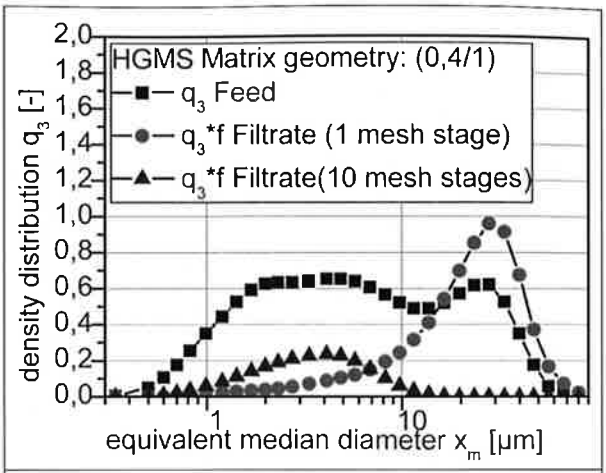

Figure 12: Density distribution of particles in the feed, density distribution q_3 multiplied by the filtrate proportion f of the filtrate for two different experiments.

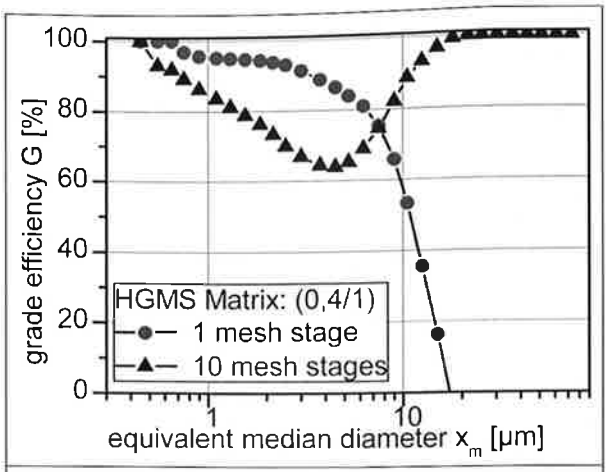

Figure 13: Grade efficiency of the test with one wire mesh stage and ten wire mesh stages.

ten units, which are mounted vertically in the filter, all particles larger than 18 µm are almost completely separated. In order to improve the separation of the remaining smaller particles, the number of mesh stages has to be increased still further.

ACKNOWLEDGEMENTS

The authors owe special thanks to all organisations and companies supporting magnetic separation at the Institute of Mechanical Process Engineering and Mechanics (MVM). Among them are Haver and Boecker OHG, PALL GmbH, Drive Technology Research Union (FVA) and the Institute of Functional Interfaces (IFG) at KIT, Campus North. The research project IGF-No. 313 ZN was supported by funds from the Federal Ministry of Economics and Technology (BMWi) through the Industrial Research Associations 'Otto von Guericke' e.V. (AiF).

REFERENCES

1. DIN IEC 61400-4: DIN IEC 61400-4 Wind turbines - Part 4: Design requirements for wind turbines gearboxes (IEC 88/354/CD:2009)/ Note: Date of issue 2010-05-10. 2010
2. Gerber R. and Birss R.R., 1983. *High Gradient Magnetic Separation*, Research Studies Press, Letchworth.
3. Kopf P., Piesche M. and Schuetz S., 2007. Beschreibung des Druckverlusts von Drahtgeweben mit Hilfe von Ähnlichkeitsgesetzen, *Filtrieren und Separieren*, **21**(6), 330-335.

A STUDY TO EXCLUDE EARTHWORMS FROM HARVESTED AND STORED RAINWATER

K.T. Oladepo[1] (koladepo1@yahoo.com), J.O. Jeje[1], O.O. Fadipe[2] and M.O. Ogedengbe[1]
[1]*Department of Civil Engineering, Obafemi Awolowo University, Ile-ife, Nigeria.*
[2]*Department of Civil Engineering, Osun State College of Technology, Esa-Oke, Osun State, Nigeria.*

People in the study area believe that rainwater, harvested and stored, would, in due course, have earthworms in it. They consider earthworms in water meant for cooking, let alone drinking, objectionable. These are the known reasons why rainwater harvesting has failed to be accepted. This study was intended to encourage dwellers of rural and semi urban communities to embrace the harvesting and storing of rainwater for domestic use and reduce their use of water from sources which potentially transmit pathogens to users. Rainfall data were collected. Dual media filters were built of palm kernel shells (PKS) over silica sand. Rainwater was harvested and passed to storage, filtered and unfiltered. During 30 days of storage the rainwater was not found to contain earthworms, although it was widely believed that it would. Passing rainwater into storage through the dual media filters produced better quality water. Any approaching earthworm would surely be filtered out.